Theory of spin torques and giant magnetoresistance in antiferromagnetic metals

A. S. Núñez,* R. A. Duine,† Paul Haney,‡ and A. H. MacDonald§
Department of Physics, The University of Texas at Austin, 1 University Station C1600, Austin, Texas 78712-0264, USA
(Received 26 April 2006; published 14 June 2006)

Spintronics in ferromagnetic metals is built on a complementary set of phenomena in which magnetic configurations influence transport coefficients and transport currents alter magnetic configurations. Here, we propose that corresponding effects occur in circuits containing antiferromagnetic metals. The critical current for order parameter orientation switching can be smaller in the antiferromagnetic case because of the absence of shape anisotropy and because spin torques can act through the entire volume of an antiferromagnet. We discuss possible applications of antiferromagnetic metal spintronics.

DOI: 10.1103/PhysRevB.73.214426 PACS number(s): 72.25.Ba, 73.43−f, 75.30.Ds, 75.50.Pp

I. INTRODUCTION

Many-electron systems can frequently be described in terms of interacting collective and quasiparticle degrees of freedom. Driving quasiparticles out of equilibrium by incorporating the system in an electronic circuit can influence the collective state. For example, inserting a superconductor in a current-carrying circuit drives the superconducting order parameter into a finite-momentum current-carrying state; the superconducting order parameter field reacts to the nonequilibrium configuration of normal metal quasiparticles that reflect off the normal/superconductor interface. Another example of this idea is spintronics in ferromagnetic metals,[1] which is based on both the dependence of resistance on magnetic microstructure[2] and on the possibility of manipulating this microstructure with transport currents.[3–10] Current effects are often largest and most robust in circuits containing ferromagnetic nanoparticles that have a spatial extent smaller than a domain wall width and therefore have magnetization dynamics that is nearly spatially coherent. In this paper, we point out that similar effects can occur in circuits containing antiferromagnetic metals. The systems that we have in mind are antiferromagnetic transition metals similar to Cr (Ref. 11) and its alloys[12] or the rock salt structure intermetallics[13] used as exchange bias materials. Both classes of material are well described by the time-dependent mean-field theory in its density-functional theory[14] setting.

Our proposal that currents can alter the micromagnetic state of an antiferromagnet may seem surprising since spin-torque effects in ferromagnets[15] are usually discussed in terms of conservation of total spin, a quantity that is not related to the staggered moment order parameter of an antiferromagnet. Spin torques are due[16] to changes in the exchange fields in a magnetic system that follow from differences between equilibrium and transport-steady-state spin densities. When the transport spin density is not parallel to the local magnetization, the exchange field contribution that it produces will drive magnetization precession. The exchange field contribution of transport electrons is usually too small to substantially alter the relative orientation of neighboring spins, but can compete with anisotropy energies and induce spatially coherent precessional orientation dynamics. In an antiferromagnet the magnetic order is staggered. It follows that only correspondingly staggered torques will drive coherent order parameter dynamics. The required torques can be produced by transport-induced spin densities that are perpendicular to the moment direction and have the host lattice periodicicity. The required alteration in torque is then produced by the alternating moment orientations in the antiferromagnet, rather than by the transport electron exchange field. Surprisingly, we find that the transverse spin densities necessary for a staggered torque occur generically in circuits containing antiferromagnetic elements.

The key observations behind our theory concern the scattering properties of a single channel containing noncollinear antiferromagnetic elements with a staggered exchange field that varies periodically along the channel and is commensurate with an underlying lattice that has inversion symmetry. As we explain in detail in Sec. II, for an antiferromagnetic element that is invariant under simultaneous spatial and staggered moment inversion it follows from flux conservation and time reversal symmetry considerations in standard one-dimensional scattering theory[17] that transmission through an individual antiferromagnetic element is spin independent, and that the spin-dependent reflection amplitude from the antiferromagnet or any period thereof has the form $\mathbf{r}=r_s 1 + r_t \mathbf{n}\cdot\vec{\tau}$, where $\mathbf{n}$ is the order parameter orientation and $\vec{\tau}$ is the Pauli spin-matrix vector; r_s and r_t are proportional to sums and differences of reflection amplitudes for incident spins oriented along and opposite to the staggered moment. The reflection amplitudes for spinors incident from opposite sides differ by changing the sign of $\mathbf{n}$ while the transmission amplitudes differ by a system specific phase factor.

We apply composition rules for transmission and reflection amplitudes, known from one-dimensional scattering theory,[17,18] to a compound circuit circuit containing paramagnetic source and drain electrodes and two antiferromagnetic elements with staggered moment orientations $\mathbf{n}_1$ and $\mathbf{n}_2$ separated by a paramagnetic spacer (see Fig. 1). A lengthy calculation whose details are not particularly illuminating proves that the transport electron spin density in the $\mathbf{n}_1 \times \mathbf{n}_2$ direction is always exactly periodic in the antiferromag-

FIG. 1. (Color online) The model heterostructure for which we perform our calculations.

nets. (A proof of this property is outlined in the Appendix.) The spin torques that appear in this type of circuit therefore *act through the entire volume of each antiferromagnet*. Physically, this result may be understood in part as a microscopic version of magnetoelectronic spin echo.[19] This analogy is incomplete, however, and does not explain the qualitative difference between in-plane and out-of-plane transport spin densities. The staggered torques on which we focus arise from out-of-plane spin densities, whereas the in-plane spin densities can be understood in terms of transport modification of the in-plane Ruderman-Kittel-Kasuya-Yosida (RKKY)-type torques that are present even in equilibrium. In ferromagnets nonequilibrium spin densities decay[15] on a length scale which is inversely related to the momentum space separation between majority and minority spin Fermi surfaces. The absence of a decay length scale for out-of-plane spin densities in the case of perfectly crystalline antiferromagnets is related in part to the absence of spin splitting in an antiferromagnetic metal's band structure. The property that out-of-plane spin densities occur in the first place can be understood in terms of the difference that occur locally in phase gradient (wave vector) between majority and minority spins. (Azimuthal spin-orientation is related to the relative phase of spin-up and spin-down components of a spinor.)

Our paper is organized as follows. In Sec. II we explain in more detail some features of the spin-dependent scattering properties of an antiferromagnet that are important for our analysis and that follow solely from symmetry considerations and are therefore completely generic. We then turn to toy-model calculations that use nonequilibrium Greens function techniques to illustrate potential consequences of giant magnetoresistance and spin-torque effects in circuits that contain only antiferromagnetic and paramagnetic elements. In Secs. III and IV we explain the model system that we study and discuss the results of our nonequilibrium Greens function calculations. We focus in this paper on what we believe to be the most favorable case, that in which the antiferromagnet has a single **Q** spin-density-wave state with **Q** in the current direction. We conclude that under favorable circumstances, both magnetoresistance and current-induced order parameter dynamics effects can be as large as the ones that occur in ferromagnets. Finally, in Sec. V we discuss some of the challenges that stand in the way of realizing these effects experimentally and briefly discuss some potential advantages of antiferromagnets over ferromagnets that would apply if materials combinations in which these effects are large and robust can be discovered.

II. SCATTERING IN SINGLE Q ANTIFERROMAGNETS

In this section we find the limitations placed by symmetry on the single-channel quasiparticle scattering matrix of a one-dimensional antiferromagnet. In an antiferromagnet the quasiparticles satisfy a Schroedinger equation with an exchange Zeeman field with oscillatory spatial dependence in the direction of the order parameter of the antiferromagnet. We assume that a single period of the spin-density wave is invariant under the combined effects of time reversal and spatial inversion. (Note that time reversal includes a spin flip in the present spin-$\frac{1}{2}$ case.) This assumption is valid for a spin-density wave that is commensurate with an underlying lattice that has inversion symmetry. The generalization from one-dimension to two or three dimensions is trivial for a single-**Q** spin-density wave state with the wave vector **Q** oriented along the current direction. An antiferromagnet circuit element composed of any integer number of spin-density-wave periods is also invariant under this symmetry operation.

We first define some notation conventions. We denote the asymptotic wave functions traveling to the right ($x\rightarrow\infty$) and to the left ($x\rightarrow-\infty$) by

$$\Psi_{-\infty}(x) = |-\infty_R\rangle e^{ikx} + |-\infty_L\rangle e^{-ikx}, \tag{1}$$

$$\Psi_{\infty}(x) = |\infty_R\rangle e^{ikx} + |\infty_L\rangle e^{-ikx}, \tag{2}$$

where $|\infty_R\rangle,\cdots$ and $|\infty_L\rangle,\cdots$ are the spinor coefficients of the right and left goers, respectively. The scattering matrix expresses the outgoing spinors in terms of the incoming spinors: $\binom{|-\infty_L\rangle}{|\infty_R\rangle}=\mathcal{S}\binom{|-\infty_R\rangle}{|\infty_L\rangle}$ with $\mathcal{S}$ in turn expressed in terms of 2×2 transmission and reflection matrices $\mathcal{S}=\binom{r\ t'}{t\ r'}$. We choose the direction of the Zeeman field in the antiferromagnet, **n**, to be the spin quantization axis. Invariance under simultaneous rotation of **n** and quasiparticle spins allows us to write each transmission and reflection matrix in the scattering matrix as a sum of a triplet and a singlet parts

$$\mathcal{S} = \mathcal{S}_s + \mathcal{S}_t \mathbf{n}\cdot\boldsymbol{\tau}. \tag{3}$$

Because the system is invariant under the space inversion-time reversal symmetry operation, the components of this transformed scattering wave functions must be related by the same scattering matrix. This condition imposes the following symmetry constraint on $\mathcal{S}$:

$$\mathcal{S}^{\dagger} = \begin{pmatrix} 0 & \sigma_y \\ \sigma_y & 0 \end{pmatrix} \mathcal{S}^{*} \begin{pmatrix} 0 & \sigma_y \\ \sigma_y & 0 \end{pmatrix}. \tag{4}$$

By rewriting this constraint explicitly in terms of the reflection and transmission matrices we obtain

$$r_s' - r_t'\tau_z = r_s + r_t\tau_z, \tag{5}$$

$$t_s - t_t\tau_z = t_s + t_t\tau_z, \tag{6}$$

$$t_s' - t_t'\tau_z = t_s' + t_t'\tau_z. \tag{7}$$

It follows that $t_t=t_t'=0$ and that $r_t'=-r_t$. The most general form of $\mathcal{S}$ allowed by this symmetry operation is

$$\mathcal{S} = \begin{pmatrix} r_s + r_t\mathbf{n}\cdot\boldsymbol{\tau} & t_s' \\ t_s & r_s - r_t\mathbf{n}\cdot\boldsymbol{\tau} \end{pmatrix}. \tag{8}$$

However, the parameter space is further constrained by unitarity. This allows us to write

$$r_s = ie^{i\nu}\sin\Theta\cos\Phi, \quad r_t = e^{i\nu}\sin\Theta\sin\Phi,$$

$$t_s' = e^{i(\nu-\xi)}\cos\Theta, \quad t_s = e^{i(\nu+\xi)}\cos\Theta, \tag{9}$$

where ξ and ν are phases that so far are independent parameters, and Θ and Φ are the polar coordinates of a sphere of

radius unity. This is the most general form for spin-dependent scattering by a integer number of periods of a one-dimensional spin-density wave. In terms of the rotation matrix $\mathcal{Q}_\Phi = \exp(i\Phi \mathbf{n}\cdot\tau)$, we obtain

$$\mathcal{S} = e^{i\nu}\begin{pmatrix} \sin\Theta\mathcal{Q}_\Phi & \cos\Theta e^{-i\xi}\mathbf{1} \\ \cos\Theta e^{i\xi}\mathbf{1} & \sin\Theta\mathcal{Q}_{-\Phi} \end{pmatrix}. \tag{10}$$

In this form, we can easily conclude that transmitted electrons will preserve their spins orientations, while reflected electrons will emerge from the system with their spin orientations rotated around the order parameter in opposite senses depending on their direction of incidence. This is to be contrasted with the case of a ferromagnetic scatterer. In that case, both the transmitted and reflected electrons are rotated, besides, the rotations are independent of the direction of incidence. As a direct consequence of these elementary, but general, considerations we reach the conclusion that single antiferromagnetic layers cannot act as spin filters, in other words, the spin polarization of a current will be conserved as it crosses an isolated antiferromagnetic element. We emphasize that while the transmission coefficients of an antiferromagnet are spin singlets, the reflection coefficient are still nontrivial, indeed for an incoming unpolarized current, while the transmitted current will be still unpolarized, the reflected current will be spin polarized along the order parameter direction. This fact is the main property that is behind the further developments to be described below.

We now briefly discuss the consequences of this result for circuits with noncollinear antiferromagnetic elements. In an array for multiple noncollinear antiferromagnets, each one will fail to induce spin polarization, however, the multiple reflection process at each interface will lead to a nontrivial spin-current configuration. Most importantly, for two antiferromagnets with respective staggered moment orientations $\mathbf{n}_1$ and $\mathbf{n}_2$ separated by an arbitrary paramagnetic spacer we are able to prove that the out-of-plane spin density, i.e., the spin density in the $\mathbf{n}_\perp \equiv \mathbf{n}_1 \times \mathbf{n}_2 / |\mathbf{n}_1 \times \mathbf{n}_2|$ direction is periodic with the lattice in the paramagnetic part of the system, and periodic with the same period as the spin density wave in the antiferromagnets. These spin densities will produce a contribution to the exchange correlation field that is out of the plane of either antiferromagnet; the average out-of-plane spin density will produce a staggered field that will drive spatially coherent precession of the antiferromagnetic order parameter and can lead to order parameter reorientation. Because the spin density is periodic in each antiferromagnet, it will not decay away from the interface in either antiferromagnet and will therefore lead to spin transfer torques that act throughout the entire volumes of the antiferromagnet elements. As we discuss later, this surprising property could potentially lead to low critical currents for induced order-parameter dynamics. A proof of this property is outlined in the Appendix. In the next sections we illustrate its consequences for spin dependent transport by performing nonequilibrium Greens function calculations on tight-binding model antiferromagnets.

III. ANTIFERROMAGNETIC METAL GIANT MAGNETORESISTANCE

The results of the previous section provide a simple way to calculate the dependence of the resistance of a circuit containing antiferromagnetic elements on the relative orientation of the order parameters, an effect that we refer to as antiferromagnetic giant magnetoresistance (AGMR). For simplicity, we consider two identical antiferromagnets with scattering matrices given by Eqs. (9) and (10), with different order parameter orientations denoted by $\mathbf{n}_1$ and $\mathbf{n}_2$. Note that throughout this paper we define $\mathbf{n}_1$ and $\mathbf{n}_2$ to be the direction of the moments opposite the spacer. We denote the distance between the antiferromagnetic layers by L. As discussed in the Appendix we calculate the scattering matrix of the compound system using standard composition rules.[17,18] The result is given by Eq. (A3):

$$|\infty_R\rangle = \mathsf{t}_2\mathsf{K}\mathsf{t}_1|-\infty_R\rangle, \tag{11}$$

where the multiple reflection kernel is defined by $\mathsf{K} = (\mathbf{1} - \mathsf{r}_1'\mathsf{r}_2)^{-1}$. The net transmission coefficient becomes:

$$\mathsf{T} = \mathrm{Tr}(\mathsf{t}_1^\dagger \mathsf{K}^\dagger \mathsf{t}_2^\dagger \mathsf{t}_2 \mathsf{K} \mathsf{t}_1). \tag{12}$$

Using Eqs. (9) and (10) we reduce it to:

$$\mathsf{T} = \cos^4\Theta\,\mathrm{Tr}(\mathsf{K}^\dagger\mathsf{K}). \tag{13}$$

The trace of the square of the multiple reflection kernel contains the information of the order parameter orientations and accounts for the dependence of the transmission on their relative orientations. Straightforward calculation leads to:

$$|\Lambda|^2 \mathrm{Tr}(\mathsf{K}^\dagger\mathsf{K}) = [2 + 4(1 + \mathbf{n}_1\cdot\mathbf{n}_2)\cos(2\nu - \delta_\mathsf{L})\cos^2\Phi\sin^2\Theta + 8\cos^4\Phi\sin^4\Theta], \tag{14}$$

where we have used δ_L to denote the phase shift associated with the translation of the antiferromagnetic layers and Λ is defined in Eq. (A6). From Eq. (14) we read off the dependence on the angle between the orientations of the order parameter that enters via $\mathbf{n}_1\cdot\mathbf{n}_2 \equiv \cos\theta$.

We see how this simple argument leads us to a finite AGMR ratio. Its precise value depends on the parameters Θ and Φ, and, when summing over momenta perpendicular to the current direction, also on their momentum dependence. To further illustrate magnetoresistive, and, in the next section, spin torque effects, we consider a specific model of an antiferromagnet in the remainder of this section.

We analyze a two-dimensional single-band lattice model intended to illustrate generic qualitative features of spintronics in antiferromagnetic metal circuits. The model has near-neighbor hopping, transverse translational invariance, and spin-dependent on-site energies, as illustrated in Fig. 1,

$$\mathcal{H}_k = -t\sum_{\langle i,j\rangle,\sigma} c^\dagger_{k,i,\sigma}c_{k,j,\sigma} + \sum_{i,\sigma,\sigma'}[(\epsilon_i + \epsilon_k)\delta_{\sigma,\sigma'} - \mathbf{\Delta}_i\hat{\mathbf{\Omega}}_i\cdot\vec{\tau}_{\sigma,\sigma'}]c^\dagger_{k,i,\sigma}c_{k,i,\sigma'}. \tag{15}$$

Here, k denotes the transverse wave number, t the hopping

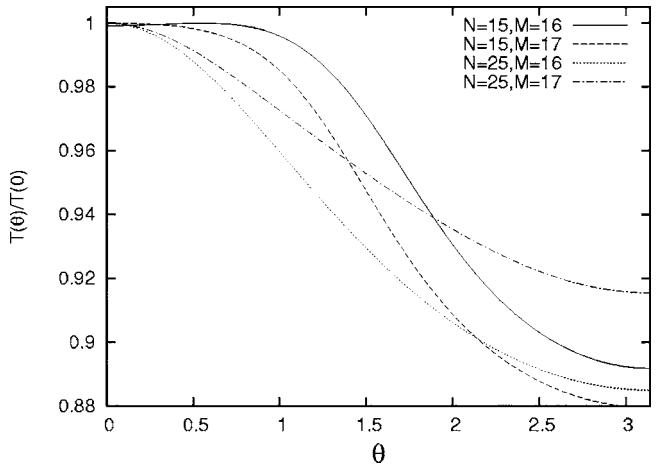

FIG. 2. Landauer-Buttiker conductance as a function of the angle θ between the magnetization orientations $\hat{\mathbf{\Omega}}_i$ on opposite sides of the paramagnetic spacer layer. There is a sizable giant magnetoresistance effect, with larger conductance at smaller θ and weak dependence on layer thicknesses. These results were obtained for $\mathbf{\Delta}/t=1$ and $\epsilon_i=0$.

amplitude and ϵ_k the transverse kinetic energy. The second term in Eq. (15) describes the exchange coupling $\mathbf{\Delta}_i$ of electrons to antiferromagnetically ordered local moments $\hat{\mathbf{\Omega}}_i = (-)^i \mathbf{n}$ that alternate in orientation within each antiferromagnet. In the paramagnetic regions of the model system $\mathbf{\Delta}_i=0$. The on-site energies ϵ_i are allowed to change across a heterojunction to represent band-offset effects.

We use the nonequilibrium Greens function formalism to describe the transport of quasiparticles across the magnetic heterostructure. The essential physical properties of the system are encoded in the real time Greens function,[18,20] defined by the ensemble average, $G^{<}_{\sigma,i;\sigma',j}(k;t,t') = i\langle c^{\dagger}_{k,i,\sigma}(t) c_{k,j,\sigma'}(t')\rangle$, from which the (spin) current and (spin) density are evaluated.

To evaluate the strength of the model's AGMR, we calculate the transmission coefficient as a function of the angle θ between orientations $\hat{\mathbf{\Omega}}_i$ on opposite sides of the spacer. In Fig. 2 the transmission coefficient is shown for specific values of the number of layers N and M, in the first and second antiferromagnet. The fact that there must be an AGMR effect can be seen by taking the limit of zero width for the paramagnetic region. In this case the resistance is greater when θ is zero since this arrangement interrupts the periodic pattern of exchange fields. The AGMR effect can generally be traced to the interference between spin current carrying electron spinors reflected by the facing layers. (This is also the origin of the spin transfer effect to be discussed later.) At the paramagnetic spacer layer thicknesses studied here, the model AGMR depends on the orientation of the layers opposite the spacer in the usual way, i.e., the resistance is highest for $\theta = \pi$ and lowest for $\theta=0$. Also, we find that the AGMR ratio, defined as the absolute difference between the maximum and minimum value of the transmission coefficient normalized to the minimum, saturates as a function of the length of the antiferromagnetic elements.

The main point of these calculations is to demonstrate by explicit calculation that AGMR in antiferromagnetic metal circuits can in principle have a magnitude comparable to GMR in ferromagnetic metal circuits. It is instructive to compare these numerical results with qualitative pictures of GMR in an effort to judge their robustness. The simplest picture of transport in a magnetic system is the bulk two-channel transport *Julliere* picture[21] in which magnetoresistance arises ultimately from the difference between the majority-spin and minority-spin resistivities of bulk material. For bulk antiferromagnets the resistivity is spin independent, so this effect cannot explain the AGMR that appears in our numerical calculations.

The difference between parallel and antiparallel configurations amounts to merely a shift by one period of the spin-density wave in the second antiferromagnet. That such a shift can give rise to AGMR is seen explicitly in Eq. (14). The sign of the AGMR for a given channel depends on the phase shift acquired in the paramagnetic spacer region by the electron. One must integrate over all such channels in the transport window, and the total AGMR is the sum over each channel's value of AGMR. Coherent interference effects are critical to seeing this effect, and we expect the AGMR ratio to vanish as the spacer thickness becomes much larger than the phase coherence length. As we explain in the discussion section, this will not be a problem in practice. We also expect that the AGMR effect will be very weak when the magnetization also varies in the plane parallel to the antiferromagnet-paramagnet interface.

IV. CURRENT-DRIVEN SWITCHING OF AN ANTIFERROMAGNET

To address the possibility of current-induced switching of an antiferromagnet we evaluate spin transfer torques in the second antiferromagnet. The spin transfer torque originates from the contribution made by transport electrons to the exchange-correlation effective magnetic field and is given[16] by $\mathbf{\Gamma} = \mathbf{\Delta}_i \hat{\mathbf{\Omega}}_i \times \langle \mathbf{s}_i \rangle / \hbar$, where $\langle \mathbf{s}_i \rangle$ is the nonequilibrium expectation value of the quasiparticle spin. (In effect, the presence of a bias voltages separates a transport window from the quasiparticle system and redirects its spin-density contribution, creating two subsystems that can mutually precess. The torque acts on the spins of quasiparticles outside the transport window while the orientations of transport spins are instantaneously fixed by the transport bias voltages and the generally noncollinear exchange fields through which they travel.) In our model system we distinguish the spin-torque component in the plane spanned by $\mathbf{n}_1$ and $\mathbf{n}_2$ and the component out of this plane. In Fig. 3 we show the in-plane and out-of-plane transport-induced spin torques. As anticipated the in-plane spin transfer torque in this model is *exactly* staggered (for any $\mathbf{\Delta}/t$ value) and is therefore extremely effective in driving order-parameter dynamics. We have checked numerically that staggered in-plane spin-transfer torques that do not decay also occur in continuum toy models of an antiferromagnet with piece-wise constant and sinusoidal exchange fields. These persistent spin torques are a generic property of antiferromagnetic circuits and related to the absence of spin splitting in the Bloch bands. The staggered in-plane spin transfer is produced by an out-of-plane spin

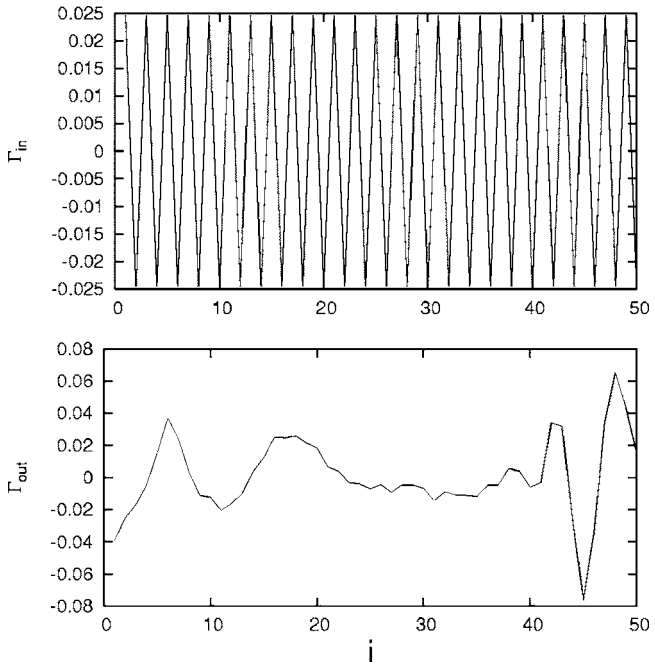

FIG. 3. Local spin-transfer torques in the downstream antiferromagnet. The in-plane spin transfer is staggered and therefore effective in driving coherent order parameter dynamics. The out-of-plane spin-transfer component is ineffective because it is not staggered. These results were obtained for $\Delta/t=1$, $\epsilon_i=0$, $\theta=\pi/2$, $N=50$, and $M=50$.

density that is *exactly* constant in our lattice model antiferromagnet and exactly periodic in a continuum model antiferromagnet.

The effect can be understood qualitatively as follows. Transport through an antiferromagnet-paramagnet interface will tend to be dominated by the top layer spin. When these spin-polarized electrons enter the second antiferromagnet the exchange field in the top layer induces a precession to an orientation that has an out-of-plane component. Exchange fields in subsequent layers produce a periodic oscillation which leaves the out-of-plane spin density at a nonzero average value. The out-of-plane spin density in the paramagnetic and upstream ferromagnetic layers has to be understood in terms of reflection from the downstream material, just as in the ferromagnetic case. While this simple explanation does not fully capture the effect since it does not capture the difference between in-plane and out-of-plane spin densities, we believe that it has some qualitative validity and can use it as a guide in anticipating the influence of the elastic, inelastic, and spin-dependent scattering that is not included in our model calculation. It is clear, for example, that as in the ferromagnetic case, the antiferromagnetic spin-torque effect will occur only if the width of the paramagnetic spacer layer is less than a spin-coherence length. On the basis of the picture explained above, we expect that the torque will act over the portion of the antiferromagnet that is within an inelastic scattering length of the interface with the paramagnetic spacer, compared to the full volume effect in the absence of scattering and the Fermi wavelength attenuation scale that applies for ferromagnets. It is also reduced when

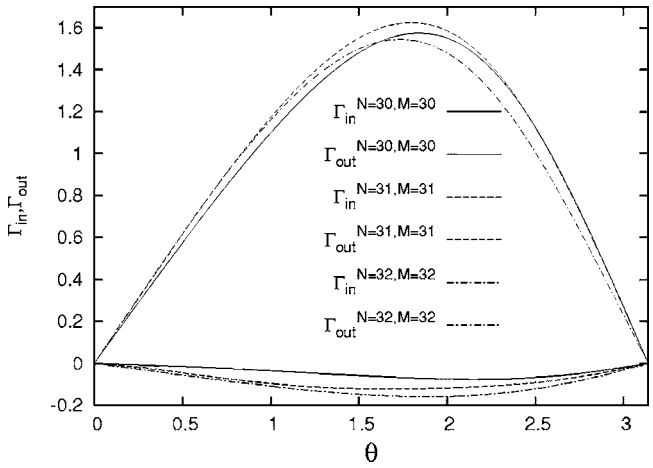

FIG. 4. Total spin transfer torque action on the downstream antiferromagnet, as a function of θ. We used the parameters $\Delta/t=1$ and $\epsilon_i=0$.

the antiferromagnetic order parameter has zero spatial average in planes perpendicular to the current direction, which is the case when antiferromagnetic domains are present.

Since the exchange interactions that stabilize the antiferromagnetic will normally be very strong compared to the transport-induce spin torques, the magnetization dynamics of each antiferromagnetic element will be coherent and respond only to the staggered component of each spin torque. In Fig. 4 we show the total staggered torque acting on the downstream antiferromagnet, as a function of the angle θ. Clearly, the out-of-plane component of the torque is small compared to the in-plane component. Since the angular dependence of the spin transfer torque is $\Gamma \sim g(\theta)\sin(\theta)$, the value for $g(\pi)$ can be extracted by evaluating $\partial_\theta \Gamma$ at $\theta=\pi$. This quantity is shown in Fig. 5, and we will see that the critical current for reversal is inversely proportional to this quantity.

Having demonstrated the presence of spin transfer torques in a heterostructure containing two antiferromagnetic elements, we estimate the critical current for switching the sec-

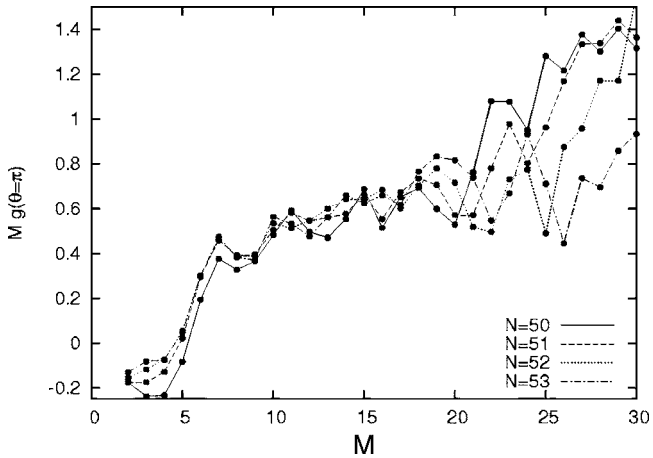

FIG. 5. Derivative of the total spin transfer torque per unit current, $Mg(\theta=\pi)$, acting on the downstream antiferromagnet with respect to the angle θ at $\theta=\pi$ as a function of M. We used the parameters $\Delta/t=1$ and $\epsilon_i=0$.

ond antiferromagnet assuming that the first is pinned. To illustrate our ideas, we use the crystalline anisotropy energy density for Cr,[11,22] given by

$$E(\mathbf{n}) = K_1(\hat{\mathbf{z}}\cdot\mathbf{n})^2 + K_2(\hat{\mathbf{x}}\cdot\mathbf{n})^2(\hat{\mathbf{y}}\cdot\mathbf{n})^2, \tag{16}$$

where $\mathbf{n}$ is a unit vector in the direction of the staggered moment and $\mathbf{Q}$ is taken to be in the $\hat{z}$ direction. The first term favors a staggered moment that is either parallel or perpendicular to the ordering vector $\mathbf{Q}$ and changes sign at the spin flop transition.[11] The term proportional to K_2 captures cubic anisotropy in the plane perpendicular to $\mathbf{Q}$.

As we have seen, the spin transfer torques act cooperatively throughout the entire antiferromagnet. We can focus our description on a single domain, characterized by the orientation of one ferromagnetic layer within the antiferromagnet since all layers will have definite relative orientations when the order parameter dynamics is spatially coherent. The order parameter equation of motion (for the downstream antiferromagnet, for example) is therefore

$$\frac{d\mathbf{n}_2}{dt} = \mathbf{n}_2 \times \left[-\frac{\gamma}{M_s}\frac{\partial E(\mathbf{n}_2)}{\partial \mathbf{n}_2} \right] + g(\theta)\omega_j \mathbf{n}_2 \times (\mathbf{n}_1 \times \mathbf{n}_2) - \alpha \mathbf{n}_2 \times \frac{d\mathbf{n}_2}{dt}. \tag{17}$$

Here, $\gamma \simeq \mu_B/\hbar$ denotes the gyromagnetic ratio, and $M_s \simeq \mu_B/a^3$ denotes the saturated staggered moment density, where $a \simeq 0.3$ nm denotes the lattice constant of Cr. The term containing $\omega_j \equiv \gamma\hbar j/(2eaM_s)$, with j the current density and e the electron charge, describes the in-plane spin transfer torque. We neglect the out-of-plane component because, as we have seen, it averages to a small value. The last term in Eq. (17) describes the usual Gilbert damping, with a dimensionless damping constant for which we take the typical value $\alpha = 0.1$.[22] The anisotropy constants are given by $K_1 = 10^3$ J m^{-3} and $K_2 = 10$ J m^{-3}.[22] Since the out-of-plane component of the spin torque competes with the anisotropy, whereas the in-plane component competes with the damping term, it turns out that (even in ferromagnets) the in-plane component of the spin torque is most important in determining the critical current for current-driven switching, providing a second justification for the neglect of this term. (Of course both terms can be calculated using standard techniques for any specific atomic and magnetic arrangement.) A linear stability analysis of Eq. (17) shows that for the optimal situation $\mathbf{n}_1 = -\hat{\mathbf{x}}$, the fixed point $\mathbf{n}_2 = \hat{\mathbf{x}}$ becomes unstable if j exceeds

$$j_c = \frac{e\alpha a}{g(\pi)\hbar}(K_1 + 8K_2) \simeq 10^5 \text{ A cm}^{-2}, \tag{18}$$

where we have taken a value for $g(\pi)$ [$g(\pi) \simeq 0.05$] from our toy model numerical calculations. In practice $g(\pi)$ will depend on the specific materials combinations in the circuit. This critical current is smaller than the typical value for current switching of a ferromagnet primarily because the spin transfer torques act cooperatively throughout the entire antiferromagnet and also because of the absence of shape anisotropy in antiferromagnets. Using the model of Eq. (17) we also find that, depending on the applied current, the staggered moment $\mathbf{n}_2$ can relax to stable fixed points at $\mathbf{n}_2 = \pm\hat{\mathbf{y}}$ or completely reverse its direction.

V. DISCUSSION AND CONCLUSIONS

The most obvious potential application of this effect is for purely antiferromagnetic spin valve structures, like those illustrated schematically in Fig. 1. Say, for example, that the circuit consists of perfectly epitaxial materials including commensurate antiferromagnets with moment alteration in the current direction and facing moments that are originally parallel. Because of the antiferromagnetic spin-torque effect, a high current can make this arrangement unstable. If we assume that the one of the two antiferromagnets is free and the other is pinned, a high current can cause a transition to a configuration in which the facing moments are antiparallel. This transition may be detected with the AGMR effect.

There are obvious challenges that make the scenario we have outlined less easy to realize than in the ferromgnetic case, even taking away the body of knowledge on ferromagnetic metal spintronics that has been built up over the past two decades. One trivial difference is that shape anisotropy can no longer be used to pin one of the ferromagnets. More challenging is the difficulty of realizing antiferromagnetic material in which the magnetization orientation of the surface layer is fixed. This aspect of antiferromagnet material physics figures prominently in efforts to increase the strength of exchange bias effects in coupled ferromagnet/antiferromagnet systems and to achieve a quantitative understanding of the behavior of exchange bias. Indeed, exchange bias might provide a useful tool for studying spin-torque effects in antiferromagnets. At a ferromagnet-antiferromagnet interface the spin orientation of the layer of an antiferromagnet that is in contact with the ferromagnet is variable because of surface roughness, domain structure in the antiferromagnet, and because of the influence of the ferromagnet on the moment arrangement within the antiferromagnet.[23] As a corollary of our ideas, we expect that a strong current will also alter the magnetic microstructure of the antiferromagnet in a hybrid heterostructure containing one pinned ferromagnetic and one antiferromagnetic element. Using the same methods as presented in the present paper, we have explicitly checked analytically and numerically that spin torques occur in such hybrid heterostructures, and we will report in more detail about these findings in a future publication. Hence, we expect that current-driven antiferromagnetic order parameter dynamics could in this case be observed by comparing exchange bias properties before and after application of a large current perpendicular to the interface.

The toy model calculations we have performed to date are all for disorder free epitaxially matched antiferromagnetic and paramagnetic elements. We expect the AGMR will be weakened by disorder, and in particular that the property that the spin transfer torque acts throughout the volume of the antiferromagnet will apply only in this idealized disorder free case. We do not, however, expect that the disorder and electron-lattice scattering that is present at room and elevated temperatures in real materials will completely destroy the

effect, but instead limit spin torques to within one mean-free path of the paramagnet-antiferromagnet interface. Using the approximate[25] universal expression for the product of resistivity ρ and mean-free-path ℓ

$$\ell\rho \approx 10^{-5}\mu\Omega\ \mathrm{cm}^2 \tag{19}$$

and taking $\rho \approx 10\ \mu\Omega$ cm for the resistivity of a typical antiferromagnetic metal gives $\ell \approx 10$ nm. Films with a thickness of 10 nm will consist typically of 50 atomic layers, close to the number chosen for our model calculations and comparable to the film thicknesses used in ferromagnetic metal spintronics circuits. We do not expect scattering to be a major obstacle to realizing this effect. Indeed, other phenomena relying on phase-coherent interference such as oscillatory exchange coupling and oscillatory GMR have been seen experimentally in ferromagnetic metallic multilayers.[24]

The materials combinations that will exhibit the effects we have in mind most strongly depend on a large variety of considerations and could be identified by a combination of experimental and theoretical work which follows in the footsteps of the successful ferromagnetic metals materials research of recent years.

In conclusion we propose that experimental and theoretical studies of the influence of current on microstructure in circuits containing antiferromagnetic metal elements will reveal interesting physics only partly anticipated in this paper, and that microstructure changes can be sensed by resistance changes.

ACKNOWLEDGMENTS

It is a pleasure to thank Jack Bass, Olle Heinonen, Chris Palmstrom, and Maxim Tsoi for helpful remarks. This research was supported in part by the National Science Foundation under Grant No. PHY99-07949, by the Welch Foundation, by DOE grant DE-FG03-02ER45958, and by a grant from the Seagate Corporation.

APPENDIX: OUTLINE OF A PROOF OF THE PERIODICITY OF THE TRANSVERSE SPIN DENSITY

In this Appendix we proof that the out-of-plane spin density is constant and equal in the left lead, spacer, and right lead of a heterostucture containing two antiferromagnets separated by a paramagnetic spacer. The proof that the out-of-plane spin density is periodic in the antiferromagnets proceeds along the same lines, but is much more involved.

The general manipulations are cumbersome when the two antiferromagnetic layers are misaligned. However, the polar representation introduced in Sec. II reduces most manipulations to standard trigonometry. We are interested in the spin densities in the regions at the left, the center (in between the scatterers), and the right, for a wave incoming from the left. We use the notation $|\pm\infty_{R/L}\rangle$ for the states at $\pm\infty$, moving to the left and right, respectively and $|0_{R/L}\rangle$ for the states at the center of the system. We need to find the combined scattering matrix of an antiferromagnetic element, a paramagnetic element, and a second antiferromagnetic element that has been translated with respect to the first and rotated in spin orientation. We first note the following behavior of scattering matrices under translation by x_0:

$$\mathsf{T}(x_0)\mathcal{S} = \begin{pmatrix} e^{2ikx_0}\mathsf{r} & \mathsf{t}' \\ \mathsf{t} & e^{-2ikx_0}\mathsf{r}' \end{pmatrix}. \tag{A1}$$

The spin-dependent scattering matrix $\mathcal{S}_{12}$ for two scatterers described by $\mathcal{S}_1 = \begin{pmatrix} r_1 & t_1' \\ t_1 & r_1' \end{pmatrix}$ and $\mathcal{S}_2 = \begin{pmatrix} r_2 & t_2' \\ t_2 & r_2' \end{pmatrix}$ is

$$\mathcal{S}_{12} = \begin{pmatrix} \mathsf{r}_1 + \mathsf{t}_1'\mathsf{r}_2\mathsf{K}\mathsf{t}_1 & \mathsf{t}_1'\mathsf{K}\mathsf{t}_2' \\ \mathsf{t}_2\mathsf{K}\mathsf{t}_1 & \mathsf{r}_2' + \mathsf{t}_2\mathsf{K}\mathsf{r}_1'\mathsf{t}_2' \end{pmatrix}, \tag{A2}$$

where we have defined the multiple reflection kernel $\mathsf{K} = (\mathbf{1} - \mathsf{r}_1'\mathsf{r}_2)^{-1}$. Using this composition rule, along with the translation property and the results explained in Sec. II for the scattering matrix of a single spatially coherent antiferromagnet in Eq. (10) [with the constraints in Eq. (9)], allows us to infer general properties of spin dependent transport through two antiferromagnets.

For the situation of an incoming beam from the left we write all amplitudes in terms of $|-\infty_R\rangle$:

$$\begin{aligned} |0_R\rangle &= \mathsf{K}\mathsf{t}_1|-\infty_R\rangle, \quad |0_L\rangle = \mathsf{r}_2\mathsf{K}\mathsf{t}_1|-\infty_R\rangle, \\ |-\infty_L\rangle &= (\mathsf{r}_1 + \mathsf{t}_1'\mathsf{r}_2\mathsf{K}\mathsf{t}_1)|-\infty_R\rangle, \\ |\infty_R\rangle &= \mathsf{t}_2\mathsf{K}\mathsf{t}_1|-\infty_R\rangle, \end{aligned} \tag{A3}$$

which solves the scattering problem at all the positions in the system. With the explicit form of the wave functions we evaluate the densities (and spin densities) at any position in the system.

$$\begin{aligned} \mathrm{S}^{\alpha}_{-\infty}(x) &= \langle -\infty_R|S^{\alpha}|-\infty_R\rangle + \langle -\infty_L|S^{\alpha}|-\infty_L\rangle \\ &\quad + \{\langle -\infty_R|S^{\alpha}|-\infty_L\rangle e^{-2ikx} + \langle -\infty_L|S^{\alpha}|-\infty_R\rangle e^{2ikx}\}, \\ \mathrm{S}^{\alpha}_{0}(x) &= \langle 0_R|S^{\alpha}|0_R\rangle + \langle 0_L|S^{\alpha}|0_L\rangle \\ &\quad + \{\langle 0_R|S^{\alpha}|0_L\rangle e^{-2ikx} + \langle 0_L|S^{\alpha}|0_R\rangle e^{2ikx}\}, \\ \mathrm{S}^{\alpha}_{\infty}(x) &= \langle \infty_R|S^{\alpha}|\infty_R\rangle + \langle \infty_L|S^{\alpha}|\infty_L\rangle \\ &\quad + \{\langle \infty_R|S^{\alpha}|\infty_L\rangle e^{-2ikx} + \langle \infty_L|S^{\alpha}|\infty_R\rangle e^{2ikx}\}. \end{aligned}$$

We split our result in spatially dependent and independent parts. First, we focus on the spatially dependent spin density in the center of the system. It is of the form

$$\{\langle 0_R|S^{\alpha}|0_L\rangle e^{-2ikx} + \mathrm{h.c.}\} = \langle -\infty_R|\mathsf{t}_1^{\dagger}\mathsf{K}^{\dagger}S^{\alpha}\mathsf{r}_2\mathsf{K}\mathsf{t}_1|-\infty_R\rangle e^{-2ikx} + \mathrm{h.c.}$$

The expectation value becomes a trace when summed over all incoming channels, while the fact that the transmissions are spin independent allows us to factor them out of the trace. We find

$$\{\langle 0_R|S^{\alpha}|0_L\rangle e^{-2ikx}\} \sim |\mathsf{t}_1|^2\{\mathsf{Tr}(\mathsf{K}^{\dagger}S^{\alpha}\mathsf{r}_2\mathsf{K})e^{-2ikx}\}.$$

The trace itself can be simplified

$$\mathsf{Tr}(\mathsf{K}^{\dagger}S^{\alpha}\mathsf{r}_2\mathsf{K}) = \mathsf{r}_2^{\mathsf{s}}\mathsf{Tr}(\mathsf{K}^{\dagger}S^{\alpha}\mathsf{K}) + \mathsf{r}_2^{\mathsf{t}}\mathbf{n}_2^{\beta}\mathsf{Tr}(\mathsf{K}^{\dagger}S^{\alpha}S^{\beta}\mathsf{K}).$$

We calculate explicitly the traces with the aid of Eq. (9). We evaluate them projecting the expression along the per-

pendicular axis using $\mathbf{n}_\perp = \mathbf{n}_1 \times \mathbf{n}_2$ and find that

$$|\Lambda|^2 \mathrm{Tr}[\mathsf{K}^\dagger(\mathbf{n}_\perp \cdot \mathbf{S})\mathsf{K}] = 4RS \sin(\chi)\sin^2\theta, \tag{A4}$$

and

$$|\Lambda|^2 \mathrm{Tr}[\mathsf{K}^\dagger(\mathbf{n}_\perp \cdot \mathbf{S})(\mathbf{n}_{1,2} \cdot \mathbf{S})\mathsf{K}] = -4\mathbf{i}RS \sin(\chi)\sin^2\theta, \tag{A5}$$

where we have introduced the denominator

$$\begin{aligned}|\Lambda(\theta,\Theta,\Phi)|^2 = {} & 1 + R^4 + 4R^2S^2 + 4R(1+R^2)S\cos\chi \\ & + 4RT[2RS + (1+R^2)\cos\chi]\cos\theta \\ & + 4R^2T^2\cos^2\theta,\end{aligned} \tag{A6}$$

with $R = \sin^2\Theta$, $T = \sin^2\Phi$, and $S = \cos^2\Phi$ characterizing the joint reflection amplitudes and the joint triplet and singlet relative weights of the reflection of the antiferromagnets, and $\chi = (2\nu - \delta_L)$ the phase shift associated with the reflections. Their identity up to a factor $-\mathbf{i}$ compensates the identity of the $\mathsf{r}^{s,t}$ up to a factor $\mathbf{i}$, and their net contribution cancels. So there is no spatially dependent part. Hence, the out-of-plane spin density is constant in the spacer.

Now, we focus on the constant parts of each expression.

$$\mathrm{S}^\alpha_{-\infty} = \langle -\infty_R|S^\alpha|-\infty_R\rangle + \langle -\infty_L|S^\alpha|-\infty_L\rangle,$$

$$\mathrm{S}^\alpha_0 = \langle 0_R|S^\alpha|0_R\rangle + \langle 0_L|S^\alpha|0_L\rangle,$$

$$\mathrm{S}^\alpha_\infty = \langle \infty_R|S^\alpha|\infty_R\rangle + \langle \infty_L|S^\alpha|\infty_L\rangle.$$

These expressions can be reduced to expressions involving only $|-\infty_R\rangle$. We obtain

$$\mathrm{S}^\alpha_{-\infty} = \langle S^\alpha + (\mathsf{r}_1^\dagger + \mathsf{t}_1^\dagger\mathsf{K}^\dagger\mathsf{r}_2^\dagger\mathsf{t}_1'^\dagger)S^\alpha(\mathsf{r}_1 + \mathsf{t}_1'\mathsf{r}_2\mathsf{K}\mathsf{t}_1)\rangle,$$

$$\mathrm{S}^\alpha_0 = \langle \mathsf{t}_1^\dagger\mathsf{K}^\dagger(S^\alpha + \mathsf{r}_2^\dagger S^\alpha \mathsf{r}_2)\mathsf{K}\mathsf{t}_1\rangle, \quad \mathrm{S}^\alpha_\infty = \langle \mathsf{t}_1^\dagger\mathsf{K}^\dagger\mathsf{t}_2^\dagger S^\alpha \mathsf{t}_2\mathsf{K}\mathsf{t}_1\rangle,$$

where the expectation value $\langle\cdot\rangle = \langle -\infty_R|\cdot|-\infty_R\rangle$. Summing over the incoming unpolarized current those expectation values become a trace

$$\mathrm{S}^\alpha_{-\infty} = \mathrm{Tr}[(\mathsf{r}_1^\dagger + \mathsf{t}_1^\dagger\mathsf{K}^\dagger\mathsf{r}_2^\dagger\mathsf{t}_1'^\dagger)S^\alpha(\mathsf{r}_1 + \mathsf{t}_1'\mathsf{r}_2\mathsf{K}\mathsf{t}_1)],$$

$$\mathrm{S}^\alpha_0 = \mathrm{Tr}[\mathsf{t}_1^\dagger\mathsf{K}^\dagger(S^\alpha + \mathsf{r}_2^\dagger S^\alpha \mathsf{r}_2)\mathsf{K}\mathsf{t}_1], \quad \mathrm{S}^\alpha_\infty = \mathrm{Tr}(\mathsf{t}_1^\dagger\mathsf{K}^\dagger\mathsf{t}_2^\dagger S^\alpha \mathsf{t}_2\mathsf{K}\mathsf{t}_1).$$

We take the difference:

$$\mathrm{S}^\alpha_0 - \mathrm{S}^\alpha_\infty = \mathrm{Tr}[\mathsf{t}_1^\dagger\mathsf{K}^\dagger(S^\alpha + \mathsf{r}_2^\dagger S^\alpha \mathsf{r}_2)\mathsf{K}\mathsf{t}_1] - \mathrm{Tr}(\mathsf{t}_1^\dagger\mathsf{K}^\dagger\mathsf{t}_2^\dagger S^\alpha \mathsf{t}_2\mathsf{K}\mathsf{t}_1), \tag{A7}$$

which can be written as

$$\mathrm{S}^\alpha_0 - \mathrm{S}^\alpha_\infty = |\mathsf{t}_1|^2 \mathrm{Tr}[\mathsf{K}^\dagger(S^\alpha + \mathsf{r}_2^\dagger S^\alpha \mathsf{r}_2 - \mathsf{t}_2^\dagger S^\alpha \mathsf{t}_2)\mathsf{K}]. \tag{A8}$$

This is easily proven to cancel when projected on the out-of-plane direction, by making use of the relations in Eqs. (A4) and (A5).

*Electronic address: alnunez@physics.utexas.edu; URL: http://www.ph.utexas.edu/~alnunez

†Electronic address: duine@physics.utexas.edu; URL: http://www.ph.utexas.edu/~duine

‡Electronic address: haney411@physics.utexas.edu; URL: http://www.ph.utexas.edu/~haney411/paulh.html

§Electronic address: macd@physics.utexas.edu; URL: http://www.ph.utexas.edu/~macdgrp

[1] S. A. Wolf, D. D. Awschalom, R. A. Buhrman, J. M. Daughton, S. von Molnr, M. L. Roukes, A. Y. Chtchelkanova, and D. M. Treger, Science **294**, 1488 (2001).

[2] M. N. Baibich, J. M. Broto, A. Fert, F. Nguyen Van Dau, F. Petroff, P. Etienne, G. Creuzet, A. Friederich, and J. Chazelas, Phys. Rev. Lett. **61**, 2472 (1988); J. Barnas, A. Fuss, R. E. Camley, P. Grunberg, and W. Zinn, Phys. Rev. B **42**, 8110 (1990).

[3] J. C. Slonczewski, J. Magn. Magn. Mater. **159**, L1 (1996).

[4] L. Berger, Phys. Rev. B **54**, 9353 (1996).

[5] M. Tsoi, A. G. M. Jansen, J. Bass, W.-C. Chiang, M. Seck, V. Tsoi, and P. Wyder, Phys. Rev. Lett. **80**, 4281 (1998); M. Tsoi, A. G. M. Jansen, J. Bass, W.-C. Chiang, V. Tsoi, and P. Wyder, Nature (London) **406**, 46 (2000).

[6] M. Tsoi, V. Tsoi, J. Bass, A. G. M. Jansen, and P. Wyder, Phys. Rev. Lett. **89**, 246803 (2002).

[7] J. Z. Sun, J. Magn. Magn. Mater. **202**, 157 (1999).

[8] E. B. Myers, D. C. Ralph, J. A. Katine, R. N. Louie, and R. A. Buhrman, Science **285**, 867 (1999); S. M. Rezende, F. M. de Aguiar, M. A. Lucena, and A. Azevedo, Phys. Rev. Lett. **84**, 4212 (2000); E. B. Myers, F. J. Albert, J. C. Sankey, E. Bonet, R. A. Buhrman, and D. C. Ralph, *ibid.* **89**, 196801 (2002); S. I. Kiselev, J. C. Sankey, I. N. Krivorotov, N. C. Emley, R. J. Schoelkopf, R. A. Buhrman, and D. C. Ralph, Nature (London) **425**, 380 (2003); W. H. Rippard, M. R. Pufall, and T. J. Silva, Appl. Phys. Lett. **82**, 1260 (2003); F. B. Mancoff, R. W. Dave, N. D. Rizzo, T. C. Eschrich, B. N. Engel, and S. Tehrani, *ibid.* **83**, 1596 (2003).

[9] Y. Ji, C. L. Chien, and M. D. Stiles, Phys. Rev. Lett. **90**, 106601 (2003).

[10] S. Urazhdin, Norman O. Birge, W. P. Pratt, Jr., and J. Bass, Phys. Rev. Lett. **91**, 146803 (2003).

[11] E. Fawcett, Rev. Mod. Phys. **60**, 209 (1988).

[12] E. Fawcett, Rev. Mod. Phys. **66**, 25 (1994).

[13] A. E. Berkowitz and K. Takano, J. Magn. Magn. Mater. **200**, 552 (1999).

[14] O. Gunnarsson and B. I. Lundqvist, Phys. Rev. B **13**, 4274 (1976).

[15] J. Z. Sun, Phys. Rev. B **62**, 570 (2000); A. Brataas, Y. V. Nazarov, and G. E. W. Bauer, Phys. Rev. Lett. **84**, 2481 (2000); X. Waintal, E. B. Myers, P. W. Brouwer, and D. C. Ralph, Phys. Rev. B **62**, 12317 (2000); X. Waintal and P. W. Brouwer, *ibid.* **63**, 220407(R) (2001); C. Heide, *ibid.* **65**, 054401 (2001); M. Stiles and A. Zangwill, *ibid.* **65**, 014407 (2001); J.-E. Wegrowe, Appl. Phys. Lett. **80**, 3775 (2002); S. Zhang, P. M. Levy, and A. Fert, Phys. Rev. Lett. **88**, 236601 (2002); G. E. W. Bauer, Y. Tserkovnyak, D. Huertas-Hernando, and A. Brataas, Phys. Rev. B **67**, 094421 (2003); M. L. Polianski and P. W. Brouwer, Phys.

Rev. Lett. **92**, 026602 (2004); A. Shpiro, P. M. Levy, and S. Zhang, Phys. Rev. B **67**, 104430 (2003); A. Fert, V. Crosa, J.-M. Georgea, J. Grolliera, H. Jaffrésa, A. Hamzica, b, A. Vaurèsa, G. Fainic, J. Ben Youssefd, and H. Le Galld, J. Magn. Magn. Mater. **272** (2004); Ya. B. Bazaliy, B. A. Jones, and S. C. Zhang, Phys. Rev. B **69**, 094421 (2004).

[16] A. S. Núñez and A. H. MacDonald, cond-mat/0403710 (unpublished).

[17] P. A. Mello and S. Tomsovic, Phys. Rev. Lett. **67**, 342 (1991); Phys. Rev. B **46**, 15963 (1992); P. A. Mello and N. Kumar, *Quantum Transport in Mesoscopic Systems* (Oxford University Press, New York, 2004).

[18] S. Datta, *Electronic Transport in Mesoscopic Systems* (Cambridge University Press, Cambridge, 1995).

[19] A. Brataas, G. Zar, Y. Tserkovnyak, and G. E. W. Bauer, Phys. Rev. Lett. **91**, 166601 (2003).

[20] C. Caroli, R. Combescot, P. Nozieres, and D. Saint-James, J. Phys. C **5**, 21 (1972).

[21] M. Julliere, Phys. Lett. **54A**, 225 (1975).

[22] E. W. Fenton, J. Phys. F: Met. Phys. **8**, 689 (1978).

[23] J. Nogues and I. K. Schuller, J. Magn. Magn. Mater. **192**, 203 (1999).

[24] S. S. P. Parkin, N. More, and K. P. Roche, Phys. Rev. Lett. **64**, 2304 (1990).

[25] J. Bass, Landolt-Bornstein New Series, Group III, Vol. 15a (Springer-Verlag, New York, 1982), pp. 139–156.